

Coupled Magnetic Cycloids in Multiferroic TbMnO_3 and $\text{Eu}_{3/4}\text{Y}_{1/4}\text{MnO}_3$

Hoyoung Jang,¹ J.-S. Lee,^{1,2} K.-T. Ko,¹ W.-S. Noh,¹ T. Y. Koo,³ J.-Y. Kim,³ K.-B. Lee,^{1,3} J.-H. Park,^{1,3,4,*}
C. L. Zhang,⁵ Sung Baek Kim,^{6,7} and S.-W. Cheong^{5,6}

¹Department of Physics, Pohang University of Science and Technology, Pohang 790-784, Korea

²NSLS Brookhaven National Laboratory, Upton, NY 11973, USA

³Pohang Acceleration Laboratory, Pohang University of Science and Technology, Pohang 790-784, Korea

⁴Division of Advanced Materials Science, Pohang University of Science and Technology, Pohang 790-784, Korea

⁵R-CEM & Department of Physics and Astronomy, Rutgers University, Piscataway, New Jersey 08854, USA

⁶I-PEM & Department of Physics, Pohang University of Science and Technology, Pohang 790-784, Korea

⁷Advancement for College Education Center, Konyang University, Chungnam 320-711, Korea.

(Received 12 August 2010; published 25 January 2011)

Based on the detailed Mn $L_{2,3}$ -edge x-ray resonant scattering results, we report a new complexity in the magnetic order of multiferroic orthomanganites, which has been considered as the simple A -type cycloid order inducing ferroelectricity. The Dzyaloshinskii-Moriya interaction involved in the orthorhombic distortion brings on F -type canting from the A type, and the ordering type becomes the off-phase synchronized bc cycloid in TbMnO_3 or the tilted antiphase ab cycloid in $\text{Eu}_{3/4}\text{Y}_{1/4}\text{MnO}_3$. The F -type canting is responsible for the magnetic field-driven multiferroicity to weak ferromagnetism transition.

DOI: 10.1103/PhysRevLett.106.047203

PACS numbers: 75.85.+t, 75.25.-j, 75.30.Et, 78.70.Ck

The discovery of large magnetoelectric effects in orthomanganite TbMnO_3 [1] has stimulated tremendous studies in multiferroicity [2,3], in which ferroelectricity and magnetism are intimately coupled, due to its great technological and fundamental importance. The magnetoelectric effects were found to be greatly enhanced especially in spiral or cycloid magnetic systems [3–6] and the noncollinear cycloid magnetism became one of the most important issues in the multiferroicity. The ferroelectricity in the magnetic cycloid is induced by unidirectional shifts of the oxygen ions to obtain an energy gain through animating Dzyaloshinskii-Moriya (DM) interaction [7,8], the so-called *inverse* DM interaction [9]. Then the relationship between the magnetic cycloid and the electric polarization was explained in the spin current model [10].

TbMnO_3 , a prototype magnetic cycloid ferroelectric system, was reported to display a variety of magnetic and electric properties [4,11–13]. Below $T_N \approx 42$ K, the system has an A -type b sinusoid order, where collinear spins on the b axis with antiparallel neighboring alignment along the c axis (A -type) modulate with a wave vector $\vec{q} = q\hat{b}$ ($q \sim 0.28$). Upon cooling through $T_C \approx 28$ K, it transits into the A -type bc -plane spin cycloid (bc cycloid) inducing ferroelectricity with electric polarization $\vec{P} = P_c\hat{c}$. The spin chirality is reversed by switching the polarization [14]. A magnetic field $\vec{H} = H_b\hat{b}$ (~ 5 T) switches the bc cycloid into the ab -plane spin cycloid (ab cycloid) with $\vec{P} = P_a\hat{a}$ [12,15]. The ab cycloid can be also realized by changing the rare-earth ions as in $(\text{Eu}, \text{Y})\text{MnO}_3$ [16,17] and $(\text{Gd}, \text{Tb})\text{MnO}_3$ [18]. The system also undergoes a first order transition into a weak ferromagnet in $\vec{H} = H_c\hat{c}$ (< 12 T) below T_C [12,16], resulting in intriguing field induced cross controls of magnetization and electric polarization [16].

The DM interaction was introduced to explain weak ferromagnetism (FM) in antiferromagnetic (AFM) materials, resulting from uniaxial F -type spin canting due to structural zigzag-type ligand shifts [7,8]. The weak FM was observed in orthorhombic A -type AFM LaMnO_3 [19], in which the DM interaction of the zigzag-type shifts in Mn-O-Mn chains induces the F -type canting. Then the DM interaction is often considered to originate either the spiral ferroelectricity or the weak FM in the orthomanganites [2]. However, considering that the orthorhombic perovskite commonly possesses the zigzag-type shifts, one can raise fundamental issues on the magnetic structure of the multiferroic orthomanganite; how the F -type canting is integrated into the A -type cycloid and which magnetic structure results from a combination of the inverse and ordinary DM interactions. Those are schematically addressed in a scenario described in Fig. 1.

Let us consider a Mn-O-Mn chain along the c axis with a transverse oxygen shift $\vec{x} = x\hat{b}$ as shown in Fig. 1(a). The superexchange interaction $H_{SE} = J\vec{S}_i \cdot \vec{S}_j$ ($J > 0$) makes the neighboring Mn spins, S_i and S_j , antiparallel (A -type). The shift \vec{x} induces the DM interaction $H_{DM} = \vec{D} \cdot \vec{S}_i \times \vec{S}_j$ through $\vec{D} = \lambda\vec{x} \times \hat{r}_{ij}$, where λ denotes the spin-orbit coupling constant and \hat{r}_{ij} is a unit vector from S_i to S_j [2,7–9]. In the A -type b sinusoid with $\vec{q} = q\hat{b}$, all spins lie on the b axis, and the local magnetic moments can be described by $\vec{m}_i^A = m_b^A \cos(\vec{q} \cdot \vec{r}_i)\hat{b}$, while in the A -type bc and ab cycloids with the spins in the bc and ab planes, they can be by $\vec{m}_i^A = m_b^A \cos(\vec{q} \cdot \vec{r}_i)\hat{b} + m_c^A \sin(\vec{q} \cdot \vec{r}_i)\hat{c}$ and $\vec{m}_i^A = m_b^A \cos(\vec{q} \cdot \vec{r}_i)\hat{b} + m_a^A \sin(\vec{q} \cdot \vec{r}_i)\hat{a}$, respectively [14]. The zigzag type shifts $\vec{x} = \pm x\hat{b}$ yield $\vec{D} = \pm D\hat{a}$. H_{DM} acts only on m_b^A and m_c^A , and contributes the F -type spin canting

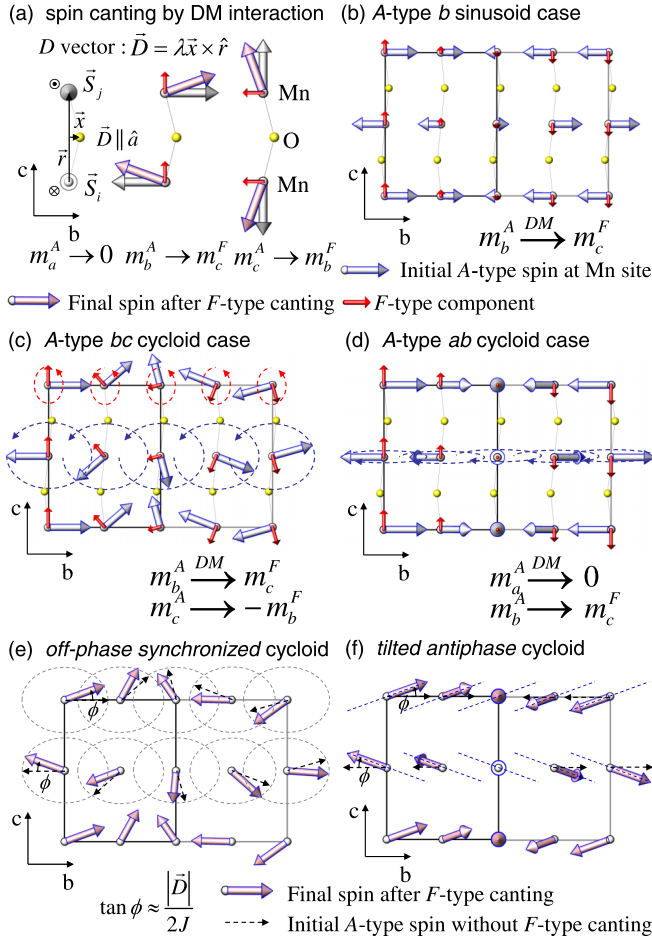


FIG. 1 (color online). (a) Spin canting by the DM interaction inducing F -type components m_c^F and m_b^F from the A-type m_b^A and m_c^A , respectively. (b)–(d) Induced F -type c sinusoid, bc cycloid, and c sinusoid for the A-type b sinusoid, bc cycloid, and ab cycloid, respectively. Resulting net spin structures; (e) off-phase synchronized cycloid and (f) tilted antiphase cycloid.

to the c and b directions, respectively, but not on m_a^A , i.e., $m_b^A \rightarrow m_c^F$, $m_c^A \rightarrow -m_b^F$, $m_a^A \rightarrow 0$. Then, the F -type order due to the spin canting is predicted to be the c sinusoid $\vec{m}_i^F = m_c^F \cos(\vec{q} \cdot \vec{r}_i) \hat{c}$ [Fig. 1(b)] or the bc cycloid $\vec{m}_i^F = -m_b^F \sin(\vec{q} \cdot \vec{r}_i) \hat{b} + m_c^F \cos(\vec{q} \cdot \vec{r}_i) \hat{c}$ [Fig. 1(c)] for the A-type b sinusoid or bc cycloid, respectively. For the A-type ab cycloid, the F -type order is the c sinusoid $\vec{m}_i^F = m_c^F \cos(\vec{q} \cdot \vec{r}_i) \hat{c}$ [Fig. 1(d)] since $m_a^A \rightarrow 0$. It is noticeable that the F type is synchronized to the A type with the same \vec{q} ($= q\hat{b}$) and chirality. Then, in the A-type bc cycloid case [Fig. 1(e)], the net spin structure becomes the off-phase synchronized cycloid with the phase difference between the c -axis neighboring spins changing from π to $\pi \pm 2\phi$ due to the unidirectional F -type canting angle ϕ of $\tan \phi \approx |D|/2J$. In the A-type ab cycloid case [Fig. 1(f)], it becomes the tilted antiphase cycloid with the cycloid planes tilted by $\pm \phi$.

To examine the scenario, we scrutinized the F -type orders using the Mn $L_{2,3}$ -edge ($2p \rightarrow 3d$) x-ray resonant

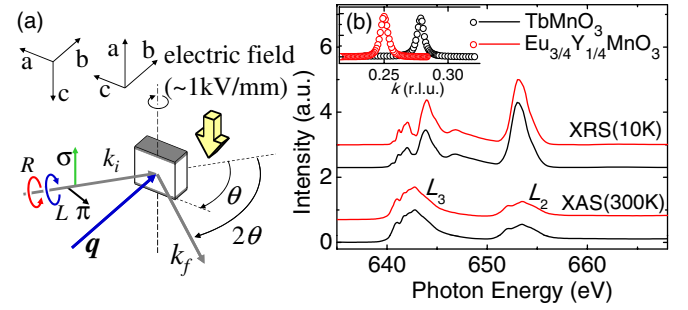


FIG. 2 (color online). (a) Scattering geometries on the bc and ab planes. (b) XRS energy profiles compared with the x-ray absorption spectra of TbMnO₃ and Eu_{3/4}Y_{1/4}MnO₃. The inset shows the F -type reflection peaks ($h\nu = 653$ eV) along $(0\ k\ 0)$.

scattering (XRS) in full combinations of the scattering geometry and the in-coming photon polarization at the 2A beam line in Pohang Light Source [20]. TbMnO₃ (A-type bc cycloid) and Eu_{3/4}Y_{1/4}MnO₃ (A-type ab cycloid) single crystals were grown by a floating zone method [4,16]. After being cut along the (010) plane and polished, the crystals were annealed for the surface recovery. \vec{P} and the chirality $\vec{C} = \sum \vec{S}_n \times \vec{S}_{n+1}$ were reversed above T_N (≈ 50 K) by an electric field ($\approx \pm 1$ kV/mm) along \hat{c} for TbMnO₃ ($\vec{P} = \pm P_c \hat{c}$) and along \hat{a} for Eu_{3/4}Y_{1/4}MnO₃ ($\vec{P} = \pm P_a \hat{a}$) [14]. After field cooling, XRS measurements were performed with warming at given temperatures maintained within 0.1 K. In the Mn K -edge ($1s \rightarrow 4p$) XRS, the F -type ($0\ 4 - q\ 0$) reflection peak appeared at the same q as the A-type ($0\ 4 - q\ 1$) one. However, it is rather vague due to its weak intensity, about 2 orders of magnitude smaller than that of the A type [21], and its origin has been disputed [22]. On the other hand, such small intensity is consistent with the small F -type ordered moment by the spin canting. The Mn $L_{2,3}$ -edge XRS, which directly accesses the magnetic $3d$ states, enhances the reflection by roughly 4 orders of magnitude and enables us to make full investigations on the F -type behaviors.

Figure 2 shows the experimental geometry and the Mn $L_{2,3}$ -edge XRS energy profile of the F -type ($0\ q\ 0$) reflection for TbMnO₃ ($q \approx 0.28$) and Eu_{3/4}Y_{1/4}MnO₃ ($q \approx 0.25$) at 10 K in comparison with the x-ray absorption spectra, which display the clean Mn³⁺ one to verify the surface quality. Both q values slightly increase above T_C [21]. The energy profile exhibits a nearly identical line shape for both systems without noticeable temperature dependence. The k scan shown in the inset clearly displays the reflection peak. Its coherence length, extracted from the peak width, is about the same as that of the A type [21], implying that both A and F types may originate from a single magnetic order. The elliptically polarized undulator beam line enables us to perform the XRS measurements for four different photon polarizations, the vertical (σ) and planar (π) linear and the right (R) and left (L) circular, without change in the geometry.

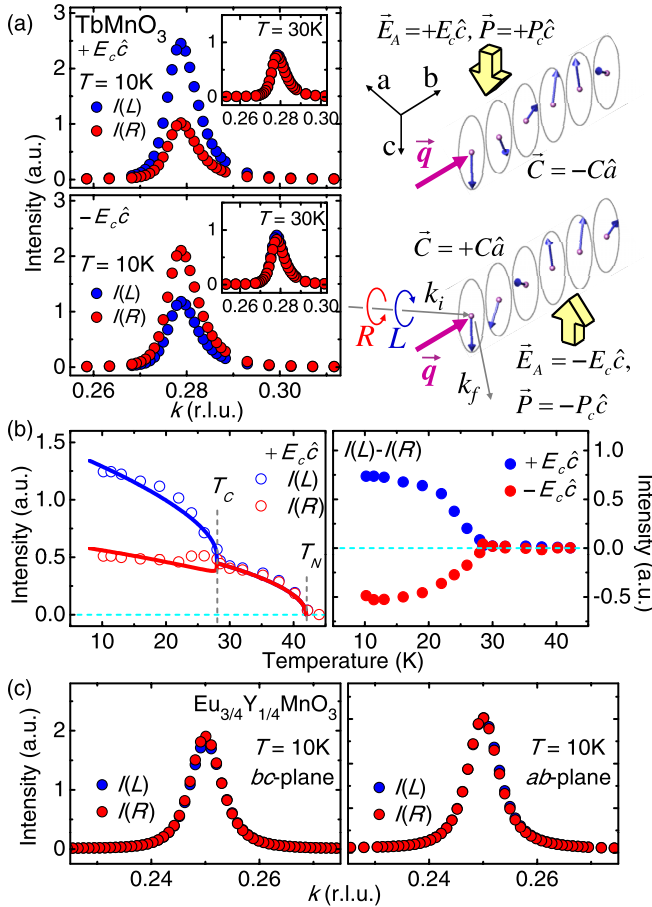


FIG. 3 (color online). (a) $I(L)$ and $I(R)$ along $(0\ k\ 0)$ in the ab -plane scattering at $h\nu = 653$ eV for E fields $\vec{E}_A = \pm E_c \hat{c}$, and (b) temperature dependence of $I(L)$ and $I(R)$ compared with calculations (solid lines) by using m_b^F and m_c^F in Fig. 4(c) and of $I(L) - I(R)$ of TbMnO_3 . (c) $I(L)$ and $I(R)$ along $(0\ k\ 0)$ in the bc - and ab -plane scattering of $\text{Eu}_{3/4}\text{Y}_{1/4}\text{MnO}_3$.

The predicted F -type order, either the cycloid or the sinusoid, can be directly examined in XRS by using the circularly polarized light. As demonstrated previously [23], the XRS intensity for the magnetic cycloid varies with the incoming photon helicity vector parallel or antiparallel to the chirality \vec{C} to yield circular dichroism. Indeed, XRS in the ab -plane scattering exhibits large circular dichroism at the F -type reflection for TbMnO_3 (A -type bc cycloid) at 10 K ($< T_C$) as shown in Fig. 3(a). The dichroism is reversed with \vec{P} switching ($\pm P_c \hat{c}$), which accompanies chirality reversal of the A -type cycloid [14], meaning the simultaneous chirality reversal (synchronized coupling) of the A -type and F -type cycloids. The dichroism gradually reduces upon heating and vanishes above T_C although the F -type signal still survives up to $T_N \approx 42$ K as shown in Fig. 3(b) [24]. No dichroism, however, was observed in the bc -plane scattering even below T_C [21], meaning $m_a^F \approx 0$. These results manifest that the F type is the noncollinear bc cycloid below T_C with the chirality reversal and becomes the collinear c sinusoid above T_C up to T_N , in contrast to a recent

proposal [26] that the F type is sinusoidal below T_C (see Ref. [25]). Meanwhile in $\text{Eu}_{3/4}\text{Y}_{1/4}\text{MnO}_3$ (A -type ab cycloid), the F -type reflection does not show any considerable circular dichroism, regardless of the scattering plane as shown in Fig. 3(c), proving that the F type is sinusoidal even below T_C . It is worth noting that all the observed F -type orders agree with the magnetic symmetry arguments, which can be described in the irreducible representations for the propagation vector $\vec{G}_k = (0, k, 0)$ in the space group Pbnm of the GdFeO_3 -type distorted orthomanganites [27]. Further, the representations show that the system also allows the G - and C -type orders [21] and suggest that the true spin structure can be a multifaceted structure displaying different types of the ordering structure, possibly observed at different reflections [11].

The cycloid order can be examined by the XRS circular dichroism, but XRS with linearly (σ and π) polarized light is necessary for quantitative analysis of the ordered magnetic moment. Figure 4 shows the ab -plane scattering results. In TbMnO_3 , the F -type reflection yields significantly enhanced $I(\pi)$ but negligible $I(\sigma)$ at $T = 30$ K ($> T_C$), while at $T = 10$ K ($< T_C$), both $I(\pi)$ and $I(\sigma)$ are finite. In $\text{Eu}_{3/4}\text{Y}_{1/4}\text{MnO}_3$, it shows large $I(\pi)$ but no $I(\sigma)$ both above and below T_C . Such intensity variations can be explained by the magnetic scattering amplitude for the electric dipole transition [28,29].

In the ab -plane scattering for a modulated ($\vec{q} = q\hat{b}$) magnetic order with the chirality $\vec{C} = \pm \hat{a}$ and scattering angle θ , the magnetic scattering intensities $I(\sigma)$, $I(\pi)$, $I(R)$, and $I(L)$ for the respective photon polarizations σ , π , R , and L can be represented as [30]

$$I(\sigma) = m_a^2 \cos^2 \theta + m_b^2 \sin^2 \theta,$$

$$I(\pi) = m_a^2 \cos^2 \theta + m_b^2 \sin^2 \theta + m_c^2 \sin^2 2\theta,$$

$$I(R) = (I(\sigma) + I(\pi))/2 \mp m_b m_c \sin \theta \sin 2\theta,$$

$$I(L) = (I(\sigma) + I(\pi))/2 \pm m_b m_c \sin \theta \sin 2\theta.$$

Here m_a , m_b , and m_c are the a -, b -, and c -axis maximum components of the local magnetic moment, respectively. Above T_C , the F type in TbMnO_3 is the c sinusoid, $\vec{m}_i^F = m_c^F \cos(\vec{q} \cdot \vec{r}_i) \hat{c}$, which yields finite $I(\pi)$ but no $I(\sigma)$. Below T_C , the bc cycloid, $\vec{m}_i^F = -m_b^F \sin(\vec{q} \cdot \vec{r}_i) \hat{b} + m_c^F \cos(\vec{q} \cdot \vec{r}_i) \hat{c}$ yields finite $I(\pi)$ and $I(\sigma)$. With $\theta \approx 27^\circ$, the ratio m_b^F/m_c^F is estimated to be about 0.7, simply inverse to that in the A -type bc cycloid [14], i.e., $m_b^F/m_c^F \approx m_c^A/m_b^A$ (ellipticity reversal). These results absolutely agree with the scenario for the F -type spin canting driven by the DM interaction of $\vec{D} = \pm D \hat{a}$, which makes contributions of $m_b^A \rightarrow m_c^F$ and $m_c^A \rightarrow -m_b^F$. The temperature dependence of both m_b^F and m_c^F , extracted from $I(\sigma)$ and $I(\pi)$, agrees well with the simple power law $(T_N - T)^{1/2}$. $m_b^F/m_c^F \approx 0.7$ also reproduces the dependence for $I(R)$ and $I(L)$ [see Fig. 3(b)]. In $\text{Eu}_{3/4}\text{Y}_{1/4}\text{MnO}_3$ with m_a^A and m_b^A , the F type maintains the c sinusoid even below T_C since $m_a^A \rightarrow 0$ and $m_b^A \rightarrow m_c^F$. Thus XRS shows a

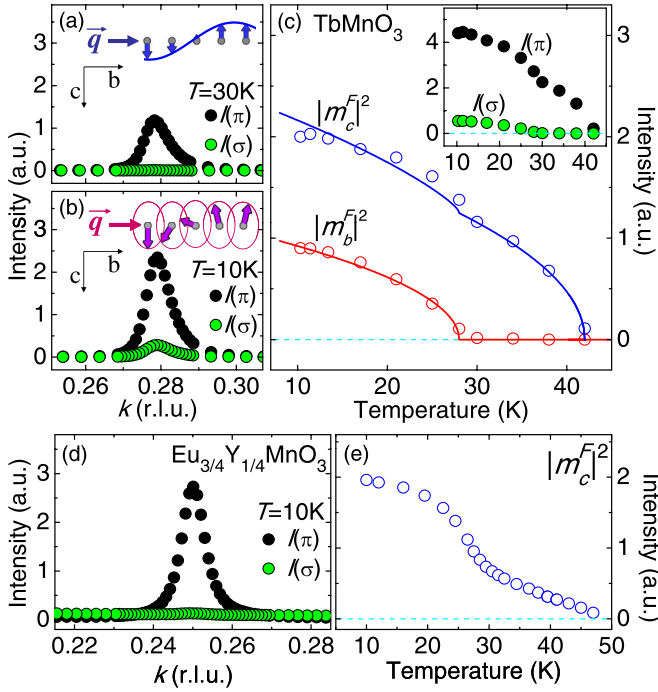


FIG. 4 (color online). The ab -plane scattering at $h\nu = 653$ eV. (a) k scan $I(\pi)$ and $I(\sigma)$ at 30 K, (b) at 10 K, and (c) temperature dependence of $|m_c^F|^2$ and $|m_b^F|^2$ (open circles) extracted from $I(\pi)$ and $I(\sigma)$ (inset) are compared with simple power law fits (solid lines) of TbMnO_3 . (d) k scan $I(\pi)$ and $I(\sigma)$ at 10 K and (e) temperature dependence of extracted $|m_c^F|^2$ of $\text{Eu}_{3/4}\text{Y}_{1/4}\text{MnO}_3$.

finite intensity only for $I(\pi)$, and $|m_c^F|^2$ is roughly proportional to $I(\pi)$ [see Fig. 4(e)]. We also note that in the bc -plane scattering, the F -type reflection has nearly the same intensity for $I(\sigma)$, $I(\pi)$, $I(R)$, and $I(L)$ in both systems above and below T_C [21], confirming that the F type involves $\vec{D} = \pm D\hat{a}$ and $m_a^F = 0$.

Considering that the shifts $\vec{x} = \pm x\hat{b}$ inducing the F type originate the weak FM in the collinear A -type AFM LaMnO_3 [19], one expects that the weak FM can be also realized in the multiferroic orthomanganites when the cycloid is released, similar to a field-driven spin structure transition in BiFeO_3 [31]. Indeed, a sufficiently large $\vec{H} = H_c\hat{c}$ derives a first order unwinding transition into the weak FM state in TbMnO_3 [12] and $\text{Eu}_{3/4}\text{Y}_{1/4}\text{MnO}_3$ [16], where the collinear A -type AFM order is stabilized and the ferroelectricity disappears. The respective ferromagnetic moments are obtained to be $0.27 \pm 0.02 \mu_B/\text{Mn}$ and $0.18 \pm 0.02 \mu_B/\text{Mn}$ at 10 K [21], which are slightly larger than and comparable to $0.18 \mu_B/\text{Mn}$ for LaMnO_3 [19]. The first order-type hysteresis behavior at the transition implies possible coexistence of the competing two phases, and the F type makes the field-induced cross controls of ferroelectricity and ferromagnetism possible [16].

In summary, we clarified the F -type magnetic orders coupled to the A -type ones in multiferroic orthomanganites using the Mn $L_{2,3}$ -edge XRS studies. The F type induced

by the DM interaction is either a cycloid or sinusoid, resulting in novel spin structures.

We thank D. R. Lee, J. Koo, B. H. Kim, and S. Y. Park for useful discussions. This work was supported by the National Creative Initiative ($c\text{CCMR}$), WCU program (R31-2008-000-10059-0), and Leading Foreign Research Institute Recruitment Program (2010-00471) through NRF funded by MEST. The work at Rutgers was supported by the DOE Grant No. DE-FG02-07ER46382. PAL is supported by POSTECH and MEST.

*Corresponding author: jhp@postech.ac.kr

- [1] T. Kimura *et al.*, *Nature (London)* **426**, 55 (2003).
- [2] S-W. Cheong and M. Mostovoy, *Nature Mater.* **6**, 13 (2007).
- [3] T. Kimura, *Annu. Rev. Mater. Res.* **37**, 387 (2007).
- [4] M. Kenzelmann *et al.*, *Phys. Rev. Lett.* **95**, 087206 (2005).
- [5] G. Lawes *et al.*, *Phys. Rev. Lett.* **95**, 087205 (2005).
- [6] K. Taniguchi *et al.*, *Phys. Rev. Lett.* **97**, 097203 (2006).
- [7] I. Dzyaloshinskii, *J. Phys. Chem. Solids* **4**, 241 (1958).
- [8] T. Moriya, *Phys. Rev.* **120**, 91 (1960).
- [9] I. A. Sergienko and E. Dagotto, *Phys. Rev. B* **73**, 094434 (2006).
- [10] H. Katsura, N. Nagaosa, and A. V. Balatsky, *Phys. Rev. Lett.* **95**, 057205 (2005).
- [11] R. Kajimoto *et al.*, *Phys. Rev. B* **70**, 012401 (2004).
- [12] T. Kimura *et al.*, *Phys. Rev. B* **71**, 224425 (2005).
- [13] N. Abe *et al.*, *Phys. Rev. Lett.* **99**, 227206 (2007).
- [14] Y. Yamasaki *et al.*, *Phys. Rev. Lett.* **98**, 147204 (2007); **100**, 219902(E) (2008).
- [15] N. Aliouane *et al.*, *Phys. Rev. Lett.* **102**, 207205 (2009).
- [16] Y. J. Choi *et al.*, *Phys. Rev. Lett.* **105**, 097201 (2010).
- [17] J. Hemberger *et al.*, *Phys. Rev. B* **75**, 035118 (2007).
- [18] Y. Yamasaki *et al.*, *Phys. Rev. Lett.* **101**, 097204 (2008).
- [19] V. Skumryev *et al.*, *Eur. Phys. J. B* **11**, 401 (1999).
- [20] J.-S. Lee *et al.*, *J. Korean Phys. Soc.* **52**, 1814 (2008).
- [21] H. Jang *et al.* (unpublished).
- [22] D. Mannix *et al.*, *Phys. Rev. B* **76**, 184420 (2007).
- [23] J. C. Lang, D. R. Lee, D. Haskel, and G. Srajer, *J. Appl. Phys.* **95**, 6537 (2004).
- [24] The small dichroism size difference with the E reversal may be due to incomplete chirality reversal or small difference in the degree of circular polarization (see Ref. [25]).
- [25] See supplementary materials at <http://link.aps.org/supplemental/10.1103/PhysRevLett.106.047203>.
- [26] S. B. Wilkins *et al.*, *Phys. Rev. Lett.* **103**, 207602 (2009).
- [27] H. W. Brinks *et al.*, *Phys. Rev. B* **63**, 94411 (2001).
- [28] J. P. Hannon, G. T. Trammell, M. Blume, and D. Gibbs, *Phys. Rev. Lett.* **61**, 1245 (1988).
- [29] J. P. Hill and D. F. McMorrow, *Acta Crystallogr. Sect. A* **52**, 236 (1996).
- [30] S. W. Lovesey and S. P. Collins, *Scattering and Absorption by Magnetic Materials* (Clarendon, Oxford, 1996).
- [31] B. Ruetter *et al.*, *Phys. Rev. B* **69**, 064114 (2004).